ELSEVIER

Journal of Fluids and Structures 21 (2005) 231–241

JOURNAL OF FLUIDS AND STRUCTURES

www.elsevier.com/locate/jfs

Investigation of the transient aerodynamic phenomena associated with passing manoeuvres

C. Noger*, C. Regardin, E. Széchényi

Institut Aérotechnique, Conservatoire National des Arts et Métiers (CNAM), 15 rue Marat, F-78210 Saint-Cyr l'École, France

Received 4 August 2004; accepted 13 May 2005
Available online 19 September 2005

Abstract

Passing manoeuvres and crosswind can have significant effects on the stability of road vehicles. The transient aerodynamics, which interacts with suspension, steering geometry and driver reaction is not well understood. When two vehicles overtake or cross, they mutually influence the flow field around each other, and under certain conditions, can generate severe gust loads that act as additional forces on both vehicles. The transient forces acting on them are a function of the longitudinal and transverse spacings and of the relative velocity between the two vehicles. Wind tunnel experiments have been conducted in one of the automotive wind tunnels of the Institut Aérotechnique of Saint-Cyr l'École to simulate the transient overtaking process between two models of a simple generic automobile shape. The tests were designed to study the effects of various parameters such as the longitudinal and transverse spacing, the relative velocity and the crosswind on the aerodynamic forces and moments generated on the overtaken and overtaking vehicles. Test results characterize the transient aerodynamic side force as well as the yawing moment coefficients in terms of these parameters. Measurements of the drag force coefficient as well as the static pressure distribution around the overtaken vehicle complete the understanding. The main results indicate the aerodynamic coefficients of the overtaken vehicle to be velocity independent within the limit of the test parameters, while unsteady aerodynamic effects appear in the case of an overtaking vehicle. The mutual interference effects between the vehicles vary as a linear function of the transverse spacing and the crosswind does not really generate any new unsteady behaviour.
© 2005 Elsevier Ltd. All rights reserved.

Keywords: Passing manoeuvres; Unsteady aerodynamics; Transient phenomena; Ground vehicle

1. Introduction

The aerodynamic design as well as the desire to reduce vehicle drag (Barnard, 1996) have made modern passenger cars more sensitive to passing manoeuvres and crosswind conditions. This sensitivity depends on the vehicle properties (mass, inertia, suspension, tires, etc.), the aerodynamic (shapes) and steering characteristics as well as on the driver reaction.

When two vehicles are driven in close proximity, they mutually influence the flow field around each other and under certain conditions they can generate severe gust loads. These loads act as additional forces on both vehicles, in

*Corresponding author. Tel.: +33 1 30 45 87 38; fax: +33 1 30 58 02 77.
E-mail address: christophe.noger@iat.cnam.fr (C. Noger).

0889-9746/$ - see front matter © 2005 Elsevier Ltd. All rights reserved.
doi:10.1016/j.jfluidstructs.2005.05.013

particular side forces and yawing moments (Takanami et al., 1974), which can alter their road holding and thus result in safety problems. Crosswind gusts also contribute to the handling qualities and lateral stability of vehicles.

Full-scale testing on road or with crosswind generators remains difficult and investigations are generally conducted on scale models in wind tunnels as either static or dynamic tests.

The passing manoeuvre processes have been analysed by many authors. Most of them relate to static testing which consists in placing one vehicle at various discrete positions relative to the other which remains fixed. Many researchers have carried out static measurements on 1/10-scale models with an emphasis on large commercial vehicles (trucks or buses). Fundamental parameters such as the longitudinal and transverse spacing (Howell, 1973), the shapes and size ratios of the models (Abdel Azim, 1994; Heffley, 1973; Yoshida et al., 1977), the ground clearance (Heffley, 1973) were studied. Measurements generally consisted of the aerodynamic forces and moments and some steady pressures. The forces were obtained either with internal strain gauge balances (Heffley, 1973; Yoshida et al., 1977) or by integrating surface pressure distributions over the vehicle (Yamamoto et al., 1997; Abdel Azim, 1994). Usually, the Reynolds number based on the model length varies between 10^5 and 6×10^5. Authors agree that it is the side force and the yawing moment that have the greatest effect on vehicle behaviour and that the longitudinal and transverse spacing have considerable importance.

Few researchers have conducted dynamic tests. These consist in moving one vehicle at different relative velocities while the other is held stationary. Yamamoto et al. (1997) made quasi-static measurements and indicated that even a small relative velocity could significantly affect the vehicle behaviour because of the duration of the action. More recently, Noger and Széchényi (2004) and Gilliéron and Noger (2004) made extensive static, quasi-static and dynamic tests and characterized the overtaking process of vehicles [Ahmed bluff bodies; Ahmed and Ramm (1984)] by varying parameters such as the longitudinal and transverse spacing, the relative velocity or the yaw angle.

The effects of a crosswind region or crosswind gusts on the transient aerodynamic coefficients were described by Yoshida et al. (1977) and Beauvais (1967), respectively.

To complete the aerodynamic measurements, some authors used flow visualization techniques and characterized the flow structures around the vehicles. Abdel Azim and Abdel Gawad (2000) and Minato et al. (1991) identified the wake structures behind the interacting vehicles, depending on the Reynolds number and on the gap flow between both vehicles (transverse spacing).

The present work describes the transient aerodynamic phenomena associated with a vehicle overtaking or overtaken by another. The aerodynamic coefficients of the overtaking/overtaken vehicle are presented as a function of the relative longitudinal position of the passing vehicle.

2. Relative velocity scaling

To be representative of the full-scale unsteady behaviour on the road, a nondimensional parameter (k) corresponding to a velocity ratio needs to be defined. It can be shown that this parameter is a ratio of the velocity of the unsteady disturbance (relative velocity V_r) to a steady velocity (V), which here is taken to be that of the vehicle causing the disturbance on the vehicle considered. The relationship between the real and experimental conditions becomes

$$k = \left.\frac{V_r}{V}\right|_{\text{Wind tunnel}} = \left.\frac{V_r}{V}\right|_{\text{Road}}. \tag{1}$$

In the same way, the aerodynamic forces are expressed with the dimensionless coefficients of drag force C_x, side force C_y and yawing moment C_n as

$$\begin{aligned} F_x &= \tfrac{1}{2}\rho S V^2 C_x(\beta), \\ F_y &= \tfrac{1}{2}\rho S V^2 C_y(\beta), \\ N &= \tfrac{1}{2}\rho S E V^2 C_n(\beta), \end{aligned} \tag{2}$$

where E denotes the model wheelbase length and S the frontal area. The relative yaw angle β is defined as the angle between the vehicle longitudinal axis and the relative wind direction. The aerodynamic forces and moments are scaled with the velocity of the vehicle causing the disturbance on the vehicle considered. This is because we consider the aerodynamic field of this vehicle (front/side pressure waves and wake) to be the source of the transient forces in question. This method is different from that of Heffley (1973) that uses a composite dynamic pressure containing the product of the two vehicles' airspeeds to take into account for the relative speed difference.

3. Experimental test bench

The experimental tests were designed to simulate the overtaking conditions between 1/5-scale models (Fig. 1). The test apparatus runs across the whole width (5 m) and length (10 m) of the wind tunnel test section (Noger and Gilliéron, 2003). It is made of a raised wooden floor (215 mm height) which houses all the test equipment and fasteners keeping the apparatus in place. The equipment consists of a linear guiding system with a belt-driven carriage and a fixed six-component unsteady aerodynamic balance. The test apparatus allows for varying the longitudinal spacing X/L (with L the model length), the transverse spacing Y/l (with l the model width), the yaw angle β, the relative velocity V_r (overtaken and overtaking motions) and the wind tunnel velocity V_{S4}. The positioning notations are shown in Fig. 2.

3.1. Positioning system

The positioning system is made of a linear guiding rail, a belt-driven carriage and a low-inertia drive facility: it is placed between the wind tunnel floor and the raised wooden floor of the test bench. A feedback controller ensures a high precision in the carriage speed and positioning. The scale model (less than 10 kg) can be carried longitudinally at speeds

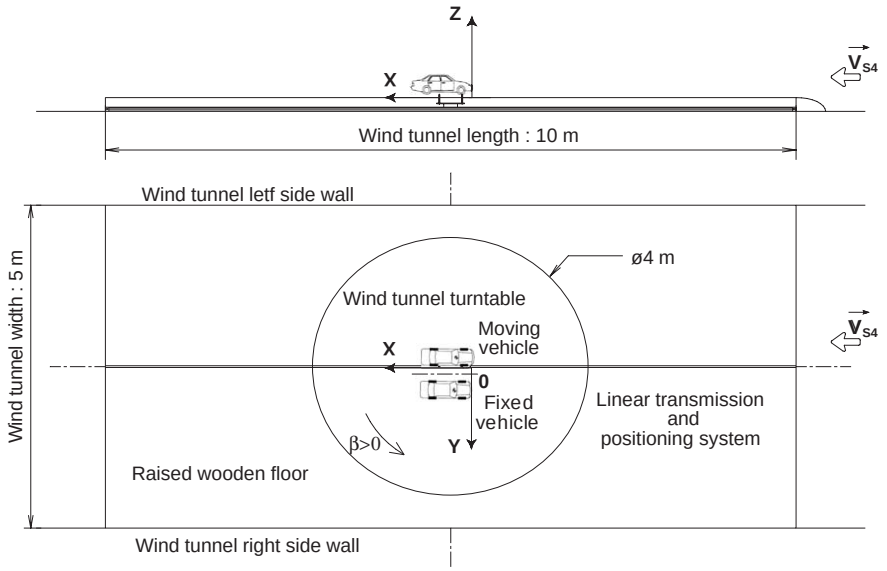

Fig. 1. Test bench layout (Noger and Gilliéron, 2003).

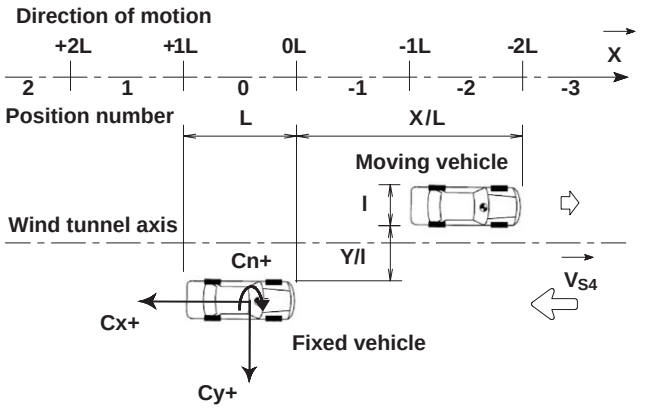

Fig. 2. Notations for the vehicle positioning.

ranging from 0 to 10 m/s with fast acceleration–deceleration ramps (up to 40 m/s^2). Due to the beginning and the end of the motion, the relative velocity is not constant during the whole process so that a trigger is used at the middle of the rail to readjust the different runs. The system is also equipped with security switches and crash protection devices. The maximum authorized stroke is 8.45 m.

When the passing vehicle travels *forward* into the wind, the measurements obtained are those on an *overtaken* vehicle while when it moves *backward* they correspond to an *overtaking* vehicle.

3.2. Unsteady aerodynamic balance

The aerodynamic balance is based on piezoelectric technology. It measures the six components of the unsteady aerodynamic forces and moments acting on the fixed vehicle. The balance is made of four three-component quartz force sensors that each measure the three orthogonal components of a force. The sensors are very stiff (high natural frequency), so that the frequency range for the present experiment was in excess of 200 Hz.

3.3. Test model

In the present tests two bluff-bodies, rounded at the leading end in the manner of Ahmed bluff-bodies (Ahmed and Ramm, 1984) were used (Fig. 3). These all had the same cross-section, but varying lengths. However, in the present paper only results concerning equal length vehicles with an aspect ratio (width-to-length) of 2.7 are reported. The passing vehicle was mounted on the belt-driven carriage, while the other was fixed to the unsteady aerodynamic balance. The ground clearance was 55 mm. Some basic experiments were made to qualify a single model whose aerodynamic characteristics are summarized in Table 1 for a wind tunnel velocity of 30 m/s and a boundary layer thickness of 20 mm.

3.4. Experimental parameters

A 16-bit data acquisition system was used to record simultaneously the characteristics of the aerodynamic forces and moments. The sampling frequency was 512 Hz and the acquisition was triggered by two position switches set along the guiding rail. All the force transducer outputs were filtered using a low-pass filter at a cutting frequency of 30 Hz.

The measurements were made with a wind tunnel velocity of 20–40 m/s which gives a Reynolds number comprised between 10^6 and 2×10^6, based on the body length. As mentioned by Heffley (1973), the effects of the boundary layer are more pronounced on the longitudinal components (drag and lift forces, pitching moment) rather than the

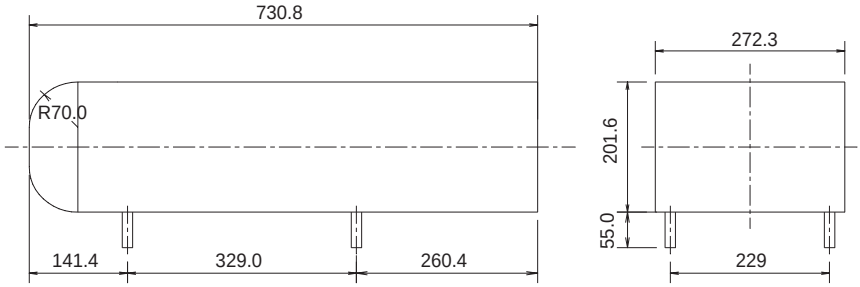

Fig. 3. Rectangular bluff body.

Table 1
Aerodynamic characteristics of a single model

β (deg)	C_x	C_y	C_n
0	0.50	0	0
10	0.51	−0.50	−0.16
20	0.48	−1.17	−0.28

lateral-directional ones (side force, rolling and yawing moments) which are the forces of primary interest in this study. Moreover, Chen (1997) indicates that there were no significant changes in the results when trying to remove the ground boundary layer thickness; so, it is left untouched in this study (about 55 mm height).

Time histories of the side force and yawing moment coefficients of the fixed vehicle are measured during the overtaken and overtaking processes. All the results are presented as a function of the relative longitudinal position of the passing vehicle rather than time. These represent only a small portion of the collected data but give trends and cover extreme situations.

The measurements reported here are made for the ranges of the various parameters summarized in Table 2. Small velocity ratios ($k \approx 0$) are assimilated to quasi-static tests and each curve corresponds to an average of 10 runs. Small differences are attributed to piezoelectric drift and experimental conditions.

4. Effect of the transverse spacing

The time histories of the aerodynamic side force and yawing moment coefficients as a function of the transverse spacing between the vehicles are shown in Figs. 4 and 5. The results are discussed only for the higher velocity ratio both for the overtaken and overtaking vehicles.

4.1. Overtaken vehicle

When the front of the passing vehicle approaches the rear end of the overtaken vehicle (Fig. 2, position no. 1), the streamlines are deflected around the front inner corner of the passing vehicle (Abdel Azim and Abdel Gawad, 2000): the increase of the static pressure on the rear left side of the overtaken vehicle is associated with sharp changes in the side force and yawing moment coefficients ($X/L = 1$).

As the transverse spacing between the vehicles diminishes, the mutual interference effects increase considerably the magnitude of the aerodynamic coefficients. Whatever the transverse spacing, the peaks occur at the same abscissa and the curves follow similar patterns. The side force coefficient changes sign when the vehicles are quasi side-by-side ($X/L \approx 0$) while the yawing moment coefficient changes sign when the passing vehicle stands near $X/L \approx 0.5$ and -0.5. Negative side force and yawing moment coefficients correspond to situations where the forces push or turn the vehicles towards each other, which can contribute to a safety problem.

Table 2
Test parameters

X/L	Y/l	β (deg)	V_r (m/s)	k
−5 to 5	0.25, 0.5, 0.7	−10, 0, 10	0.2 to 10	0.007 to 0.5

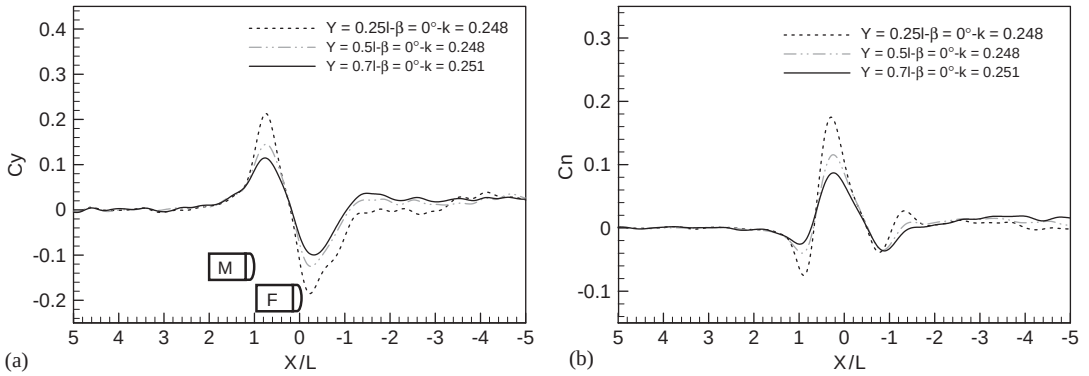

Fig. 4. Effect of the transverse spacing on the coefficients of (a) side force and (b) yawing moment for the overtaken vehicle.

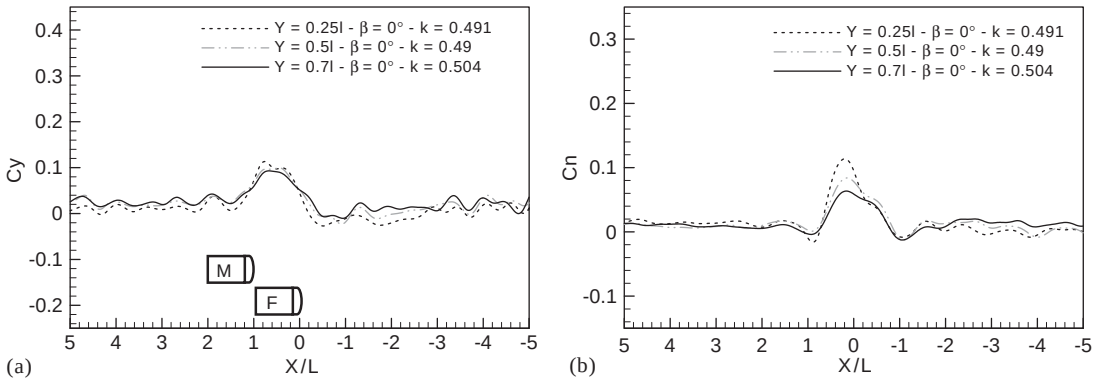

Fig. 5. Effect of the transverse spacing on the coefficients of (a) side force and (b) yawing moment for the overtaking vehicle.

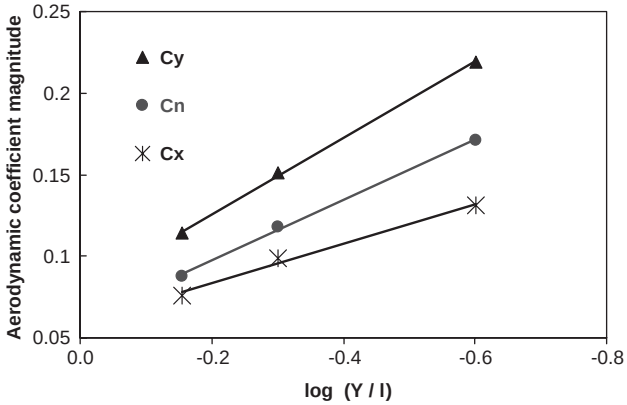

Fig. 6. Variation of the aerodynamic coefficient magnitudes with the transverse spacing.

In both cases, the magnitudes of the side force and yawing moment coefficients vary quasi-linearly as a function of the log of the transverse spacing (Fig. 6).

4.2. Overtaking vehicle

Fig. 5 shows that the unsteady effects on an overtaking vehicle, discussed above, make the influence of the transverse spacing very much smaller. The overtaking vehicle is less sensitive to the transverse spacing than the overtaken vehicle.

5. Effect of the relative velocity

Three relative velocities are chosen and compared with the quasi-static tests for the smallest transverse spacing. The resulting disturbances are at frequencies ranging from 3.5 to 14 Hz. One must already note that static ($k = 0$) and quasi-static (k small) measurements give similar trends (Noger, 2002) so that quasi-static measurements were adopted to compare with dynamic ones. The *forward* and *backward* movements of the passing vehicle are associated with an *overtaken* and *overtaking* vehicle, respectively. It must also be noted that as the front and rear ends of the models do not have the same shape, there is also a shape influence in the comparison between the overtaking and the overtaken processes, but this is not discussed here.

5.1. Overtaken vehicle

Fig. 7 shows the aerodynamic coefficients to be independent of the relative velocity up to a reduced frequency of at least 0.25: the time histories are almost identical, indicating that the unsteady phenomena are negligible. The highest velocity ratio of the tests ($k \approx 0.25$) shows only small unsteady effects when compared with the quasi-static case ($k \approx 0$). Both aerodynamic coefficients switch sign as the passing vehicle reaches and passes the overtaken one.

5.2. Overtaking vehicle

The time histories of the side force and yawing moment coefficients (Fig. 8) show the aerodynamic behaviour of the overtaking vehicle to be somewhat different from that of the overtaken vehicle. The aerodynamic coefficients become velocity dependent for $k \geqslant 0.2$.

For the highest velocity ratio, the transient side force and yawing moment coefficients are considerably reduced as compared to their quasi-steady values. There is also a time lag that increases with an increase in the velocity ratio. This is in good agreement with the results of Tsuei and Savas (2000) who obtained similar trends when studying their platoon.

6. Effect of the crosswind

The effect of the yaw angle (crosswind) on the aerodynamic coefficients is shown for both the overtaken and overtaking vehicles. Symmetrical yaw angles (-10° and 10°) are chosen for comparison with the zero yaw angle case (no crosswind, dotted line) only for the smallest transverse spacing. The mean values (± 0.4 and ± 0.15, respectively, for

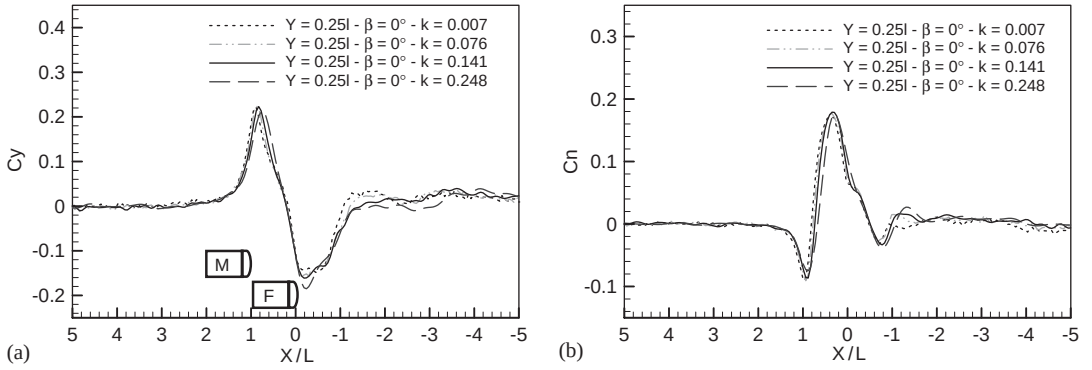

Fig. 7. Effect of the relative velocity on the coefficients of (a) side force and (b) yawing moment for the overtaken vehicle.

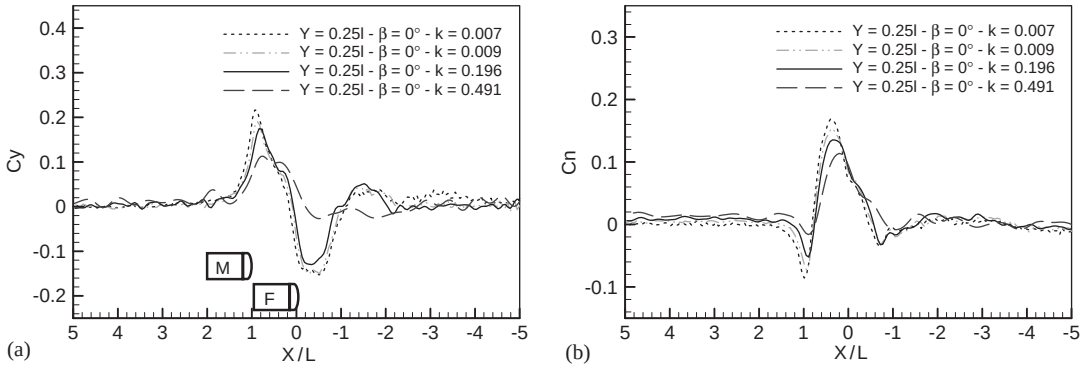

Fig. 8. Effect of the relative velocity on the coefficients of (a) side force and (b) yawing moment for the overtaking vehicle.

$C_y(\pm 10^\circ)$ and $C_n(\pm 10^\circ)$) have been subtracted to show the part due to the passing manoeuvres. At positive yaw angles, the fixed vehicle is upwind of the passing vehicle (refer Fig. 1).

6.1. Overtaken vehicle

The trends of the side force and yawing moment coefficients (Fig. 9) are quite similar for the three yaw angles, indicating that the crosswind does not really affect the overtaken vehicle behaviour as long as it remains relatively small.

6.2. Overtaking vehicle

Fig. 10 shows the side force and yawing moment variations of the overtaking vehicle. As in the case of Fig. 8, the coefficients are velocity dependent. Even far upstream (position no. −5) the wake of the moving vehicle interacts with that of the overtaking vehicle.

7. Drag force coefficient

Fig. 11 shows the evolution of the drag force coefficient with the longitudinal and transverse spacings. As indicated in Section 4.1, the drag force coefficient also varies quasi-linearly as a function of the log of the transverse spacing (Fig. 6). Note that the mean value of the drag force coefficient (0.38) has been subtracted to show the part due to the passing manoeuvres. This mean value is quite different from that of Table 1 because of the ground boundary layer thickness.

The drag force coefficient of the overtaken vehicle increases gradually as the passing vehicle approaches. The first minimum is initially reached when the high-pressure field at the front of the passing vehicle tends to increase the base pressure of the overtaken vehicle (i.e. the front of the passing vehicle stands at the rear end of the overtaken vehicle,

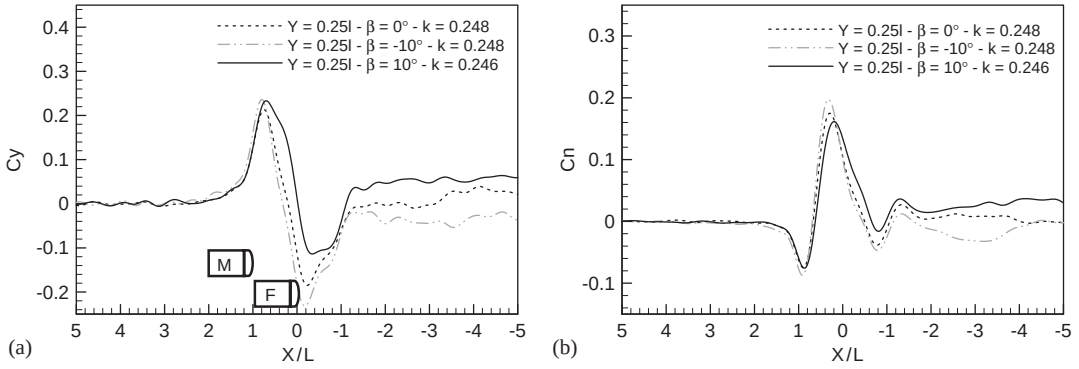

Fig. 9. Effect of the crosswind on the coefficients of (a) side force and (b) yawing moment for the overtaken vehicle.

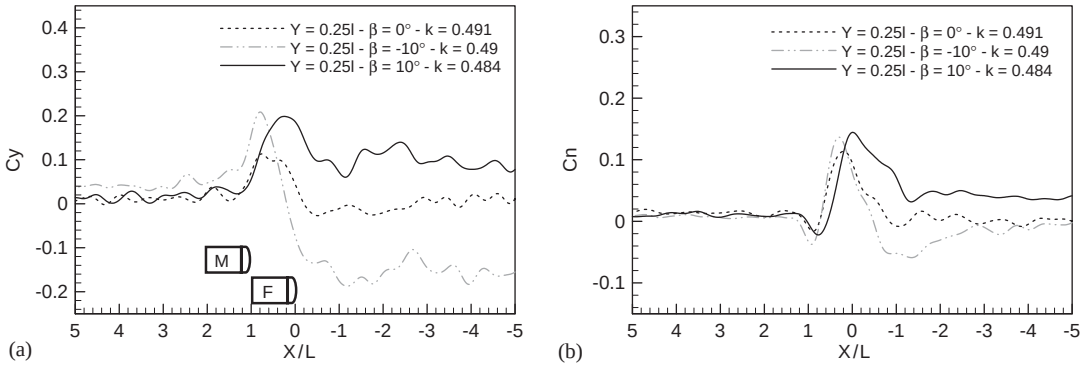

Fig. 10. Crosswind effects on the coefficients of (a) side force and (b) yawing moment for the overtaking vehicle.

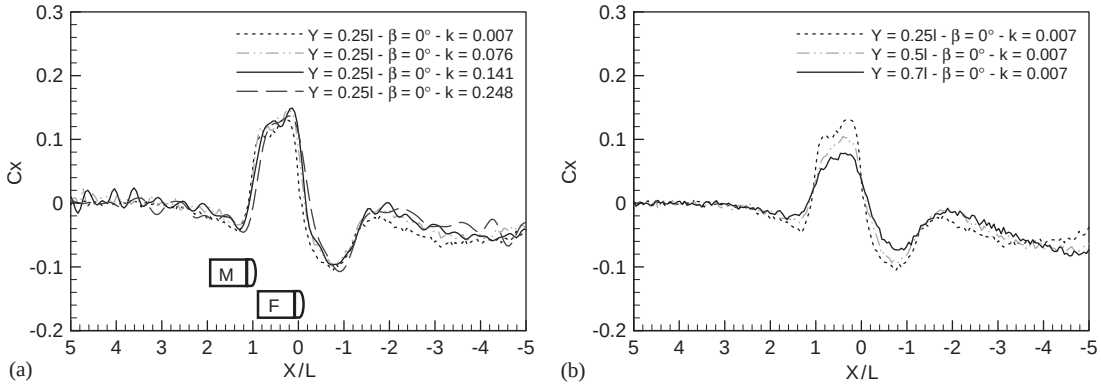

Fig. 11. Effect of the longitudinal and transverse spacings on the drag force coefficient for the overtaken vehicle.

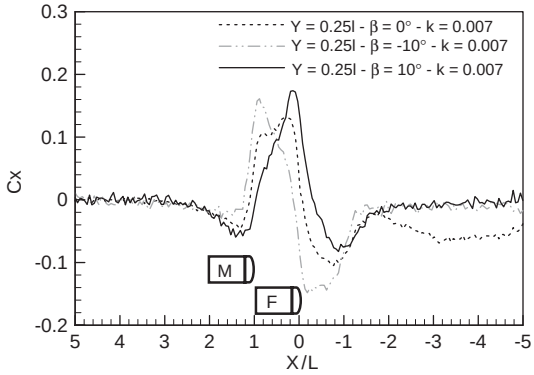

Fig. 12. Crosswind effects on the drag force coefficient for the overtaken vehicle.

position no. 1). The drag coefficient increases to its maximum value when both vehicles are quasi side-by-side. Finally, the second minimum is reached when the rear end of the passing vehicle is aligned with the front end of the overtaken vehicle (position no. −1).

Even far upstream, the wake of the passing vehicle interacts with that of the overtaken vehicle which does not recover the value of a single vehicle. Moreover, Fig. 12 indicates the drag of the overtaken vehicle to be less affected by the overtaking vehicle when there is crosswind.

8. Static pressure distribution

To complete our understanding, the static pressure coefficient around the overtaken vehicle is discussed for the static case. There is no crosswind, the velocity ratio k is 0 and the transverse spacing is $0.25l$. From the dynamic measurements, three discrete relative longitudinal positions of the passing vehicle are compared with the values of a single vehicle ($X/L = 5$): respectively, 0.75, 0.5 and $0.25L$. The static pressure coefficient is defined by

$$C_p = \frac{P_s - P_{s\infty}}{(1/2)\rho\, V_{S4}^2}, \tag{3}$$

where $P_{s\infty}$ is the static pressure reference of the wind tunnel and V_{S4} the wind tunnel velocity (30 m/s). Fig. 13 shows the static pressure distribution measured at mid-height around the overtaken vehicle for the three abscissae in comparison with that of a single vehicle. IS denotes the inner side of the fixed vehicle (i.e. left side of the overtaken vehicle) while OP denotes its outer side.

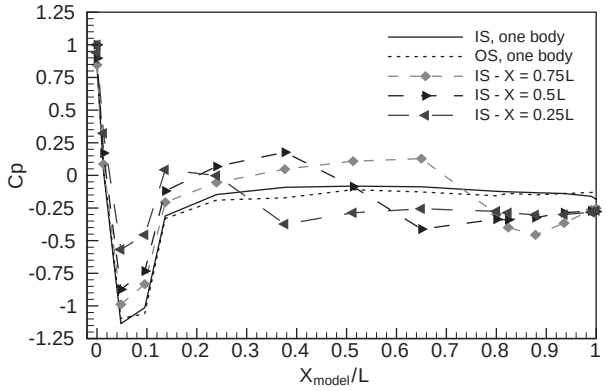

Fig. 13. Static pressure coefficient around the overtaken vehicle for three discrete positions of the overtaking vehicle.

When only one vehicle is considered, the inner and outer sides are typically symmetrical. As the relative longitudinal spacing reduces between the vehicles, the interaction progresses along the overtaken vehicle on the inner side. The passing manoeuvre generates an asymmetrical flow around the body, which is at the origin of the appearance of the forces and moments. This is confirmed by the static pressures of the outer side which are not (or little) affected by the flow-field changes, all the OS curves coincide with that of the single vehicle (not shown for clarity).

9. Conclusion

The transient aerodynamic phenomena associated with passing manoeuvres, with or without crosswind, were studied.

In the tests reported here, two simplified bluff bodies (simple generic automobile shapes) were used: one was mounted on a belt-driven carriage (passing vehicle) while the other was fixed to a stationary unsteady aerodynamic balance. Various parameters were studied, such as the longitudinal X/L and transverse Y/l spacings, the relative velocity V_r (overtaken and overtaking motions) and the yaw angle β. The aerodynamic coefficients were normalized with the velocity of the vehicle causing the disturbance on the considered vehicle.

The side force coefficient sharply increases or decreases as the passing vehicle approaches, respectively, the rear and front ends of the overtaken vehicle ($X/L = 1$ or -0.5) while for the yawing moment coefficient this occurs when the front and rear ends of the passing vehicle are at the mid-length of the overtaken vehicle ($X/L = 0.5$ and -0.5). The drag force and yawing moment coefficients indicate the most significant interactions to appear when the passing vehicle stands in the range of $1 \leqslant X/L \leqslant -1$. The static pressure distribution shows the inner side of the overtaken vehicle to be affected by the passing manoeuvres while the outer side remains little perturbed.

In the case of the overtaken vehicle, the aerodynamic coefficients are velocity independent within the limits of the test parameters, although small differences do appear for the highest velocity ratio. The interference phenomenon can then be considered as quasi-steady. In the case of the overtaking vehicle, unsteady aerodynamic effects appear at high velocity ratios and generate lower aerodynamic coefficients on the overtaking vehicle than those of the quasi-static tests. In these cases there is also a time lag corresponding to the time for the disturbed vehicle to return to the nonperturbed state.

The mutual interference effects considerably increase the aerodynamic coefficients as the transverse spacing diminishes between the vehicles: a 50% increase is observed in the magnitude of the aerodynamic coefficients of side force and yawing moment. The whole aerodynamic coefficients vary quasi-linearly as a function of the logarithm of the transverse spacing. The crosswind effects ($-10^\circ < \beta < 10^\circ$) do not really generate any new unsteady effects either when overtaking or being overtaken.

Although a good deal of data had been analysed, there is still much to be understood on these transient aerodynamic phenomena, and further investigations are needed to predict them. The next step in this work will be to analyse the data relative to the influence of the front shapes and sizes (aspect ratios) of the vehicles on each other's aerodynamic fields.

References

Abdel Azim, A.F., 1994. An experimental study of the aerodynamic interference between road vehicles. SAE paper no. 940422.

Abdel Azim, A.F., Abdel Gawad, A.F., 2000. A flow visualization of the aerodynamic interference between passenger cars. SAE paper no. 2000-01-0355.

Ahmed, S.R., Ramm, G., 1984. Some salient features of the time-average ground vehicle wake, SAE Technical paper 840300 Inc., pp. 1–31.

Barnard, R.H., 1996. Road Vehicle: Aerodynamic Design. A.W. Longman Limited, New York.

Beauvais, F.N., 1967. Transient nature of wind gusts effects on an automobile. SAE paper no. 670608, pp. 2219–2225.

Chen, A.L., 1997. Experimental investigation of transient aerodynamics in vehicle interactions. Ph.D. Dissertation, University of California, Berkeley, USA.

Gilliéron, P., Noger, C., 2004. Contribution to the analysis of transient aerodynamic effects acting on vehicles. SAE paper no. 2004-01-1311.

Heffley, R.K., 1973. Aerodynamics of passenger vehicles in close proximity to trucks and buses. SAE paper no. 730235, pp. 901–914.

Howell, J.P., 1973. The influence of the proximity of large vehicle on the aerodynamic characteristics of a typical car. Advances in Road Vehicle Aerodynamics, In: Bhra, H.S. (Ed.), Fluid Engineering, pp. 207–221.

Minato, K., Ryu, H., Kobayashi, T., 1991. Aerodynamics of vehicles in tunnels—flow visualizations using the laser light sheet method and its digital image processing. SAE paper no. 910314, pp. 123–131.

Noger, C., 2002. Étude expérimentale des phénomènes aérodynamiques apparaissant lors du processus transitoire de dépassement de deux véhicules, IAT-CNAM report 2446/A.

Noger, C., Gilliéron, P., 2003. Banc expérimental d'analyse des phénomènes aérodynamiques automobiles. 16th French Mechanical Congress (CFM), Nice, September 1–5.

Noger, C., Széchényi, E., 2004. Experimental study of the transient aerodynamic phenomena generated by vehicle overtaking. Eighth International Conference on Flow-Induced Vibration (FIV), Ecole Polytechnique, Paris, July 6–9.

Takanami, K., Sakai, T., Matsushita, A., 1974. Measurement of transient aerodynamic forces and some consideration of their effects when a vehicle passes side wind blower. Bulletin of JSAE 6.

Tsuei, L., Savas, O., 2000. A wind tunnel investigation of the transient aerodynamic effects on four car platoon during passing maneuvers, SAE paper no. 2000-01-0785.

Yamamoto, S., Yanagimoto, K., Fukuda, H., China, H., Natagawa, K., 1997. Aerodynamic influence of a passing vehicle on the stability of the other vehicle. JSAE Review 18, 39–44.

Yoshida, Y., Muto, S., Imaizumi, T., 1977. Transient aerodynamic forces and moments on models of vehicles passing through a crosswind. SAE Technical paper series no. 770391, pp. 1–14.